FERMILAB-PUB-23-162-SQMS

MAGPI: Measurement of Axion Gradients with Photon Interferometry

Michael A. Fedderke[1,*] Jedidiah O. Thompson[2,†] Raphael Cervantes[3] Bianca Giaccone[3] Roni Harnik[4,5] David E. Kaplan[1] Sam Posen[3] and Surjeet Rajendran[1]

[1] *The William H. Miller III Department of Physics and Astronomy, The Johns Hopkins University, Baltimore, Maryland 21218, USA*
[2] *Stanford Institute for Theoretical Physics, Stanford University, Stanford, California 94305, USA*
[3] *Fermi National Accelerator Laboratory, Batavia, Illinois 60510, USA*
[4] *Theory Division, Fermi National Accelerator Laboratory, Batavia, Illinois 60510, USA*
[5] *Superconducting Quantum Materials and Systems Center (SQMS), Fermi National Accelerator Laboratory, Batavia, Illinois 60510, USA*

(Dated: April 19, 2023)

We propose a novel search technique for axions with a CP-violating monopole coupling $\tilde{g}_Q$ to bulk SM charges $Q \in \{B, L, B-L\}$. Gradients in the static axion field configurations sourced by matter induce achromatic circular photon birefringence via the axion–photon coupling $g_{\phi\gamma}$. Circularly polarized light fed into an optical or (open) radio-frequency (RF) Fabry–Pérot (FP) cavity develops a phase shift that accumulates up to the cavity finesse: the fixed axion spatial gradient prevents a cancellation known to occur for an axion dark-matter search. The relative phase shift between two FP cavities fed with opposite circular polarizations can be detected interferometrically. This time-independent signal can be modulated up to non-zero frequency by altering the cavity orientations with respect to the field gradient. Multi-wavelength co-metrology techniques can be used to address chromatic measurement systematics and noise sources. With Earth as the axion source, we project reach beyond current constraints on the product of couplings $\tilde{g}_Q g_{\phi\gamma}$ for axion masses $m_\phi \lesssim 10^{-5}\,\text{eV}$. If shot-noise-limited sensitivity can be achieved, an experiment using high-finesse RF FP cavities could reach a factor of $\sim 10^6$ into new parameter space for $\tilde{g}_Q g_{\phi\gamma}$ for masses $m_\phi \lesssim 10^{-10}\,\text{eV}$.

Introduction.—Axions[1] are compelling extensions to the Standard Model (SM) that can address the strong CP problem [1–3], behave as quintessence fields [4, 5] or dark-matter (DM) candidates [6, 7], or simply be other light degrees of freedom expected from UV theory [8, 9].

An axion ϕ generically couples to photons, $\mathcal{L} \supset -g_{\phi\gamma}\phi F\tilde{F}/4$, inducing circular photon birefringence [10–13]. Oppositely handed photons propagating in a varying axion field pick up light-frequency-independent (achromatic) phase shifts $\alpha_\pm$ of opposite signs, which depend only on the difference $\Delta\phi$ in the axion field value at the endpoints of the photon path: $\alpha_\pm = \pm g_{\phi\gamma}\Delta\phi/2$. A large body of literature exists on the phenomenology of this effect in cosmological [14–40], astrophysical [25, 41–45], and lab-based contexts [46–51].

In general, axions can also have monopole couplings $\tilde{g}_Q$ to bulk SM matter charges Q: e.g., to baryon number B via $\mathcal{L} \supset -\tilde{g}_B\phi\bar{N}N$, where N is a nucleon field. Such couplings source static axion field gradients around ordinary objects, with a range $r_\phi \sim 1/m_\phi$ set by the axion mass m_ϕ. This scenario, while violating both CP and the axion shift symmetry, arises naturally for a QCD axion in the presence of a nonzero strong Θ angle [52, 53], and for general axions has been invoked as an environmental explanation for the $(g-2)_\mu$ anomaly [54, 55]. A light axion with such couplings may involve a mass tuning, but this depends on the UV cutoff and other assumptions.

[1] In this work, the term "axion" is used to refer to either the QCD axion or axion-like particles (ALPs), as appropriate.

The presence of both couplings, $g_{\phi\gamma}$ and $\tilde{g}_Q$, is commonly referred to as the 'monopole–dipole' scenario. Of course, independent constraints on both $g_{\phi\gamma}$ and $\tilde{g}_Q$ exist. Bounds on $g_{\phi\gamma}$ arise from many phenomena [56–68]: for example, astrophysical bodies could emit axions which may also convert to photons in magnetic fields. Axion–photon interconversion would also cause spectral distortions of sources. The strongest bounds are $g_{\phi\gamma} \lesssim 6 \times 10^{-13}\,\text{GeV}^{-1}$ for $m_\phi \lesssim 10^{-11}\,\text{eV}$ [61]. Monopole couplings $\tilde{g}_Q$ induce fifth forces stringently constrained by, e.g., tests of the weak equivalence principle [69–76]: $\tilde{g}_B \lesssim 6 \times 10^{-25}$ for $m_\phi \lesssim 1/R_\oplus \sim 3 \times 10^{-14}\,\text{eV}$ [75], with bounds on $\tilde{g}_L$ and $\tilde{g}_{B-L}$ being of similar magnitude.

In this paper, we propose an interferometric laboratory experiment that we estimate to be capable of probing new parameter space for the product of couplings $\tilde{g}_Q g_{\phi\gamma}$. The idea is summarized in Fig. 1. A Michelson interferometer with rigid, high-finesse Fabry–Pérot (FP) cavities of length ℓ in its arms is set up such that those arms are fed with light of opposite circular polarization. In the presence of a static axion field gradient sourced by nearby matter, a time-independent, achromatic phase shift develops between the two arms. A laboratory mass could be the axion source, but the strongest accessible source is generally Earth, which for $Q = B$ gives a vertical surface field gradient $|\nabla\phi|_\oplus \sim 0.2\,\text{eV}^2 \times \tilde{g}_B/(6 \times 10^{-25})$ for $m_\phi \lesssim 1/R_\oplus$ (for $Q = L$ or $B - L$, $|\nabla\phi|_\oplus$ is smaller by a factor of ~ 2). To be sensitive to this gradient, the cavities should be oriented vertically.

Crucially for this setup, the phase shifts in the interferometer arms accumulate linearly with cavity finesse $\mathcal{F}$.

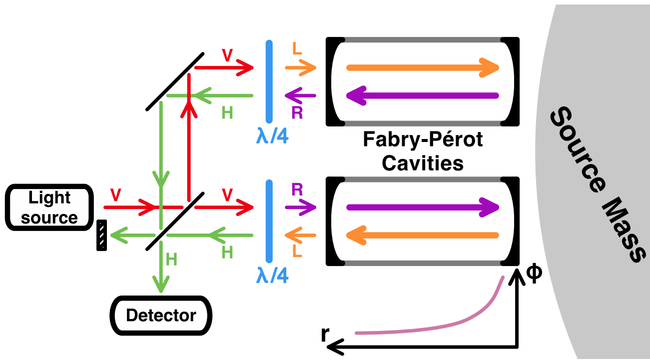

FIG. 1. The proposed experiment. Vertically polarized (V) light (optical or RF) is phase modulated and split into two beams, which are passed through oppositely oriented quarter-wave plates to become right- (R) and left- (L) circularly polarized, respectively. The circular polarizations are fed into rigid, high-finesse FP cavities, where they accumulate a phase shift from the axion field gradient sourced by a nearby mass (e.g., Earth, or a small laboratory mass). Finally, the beams pass back through the $\lambda/4$-plates to become horizontally polarized (H) and are interfered at the beamsplitter. Signal detection is via a carrier–sideband beat note at the dark port.

Photon helicity flips on reflection at each end of the cavity; if uncompensated, this would cause the phase shifts for outbound and return trips in the cavity to have opposite signs, leading to a round-trip signal cancellation [47]. However, that sign change is exactly compensated for by $\Delta\phi$ changing sign for trips in opposite directions in a static field gradient. The signal thus does not cancel, and can be boosted by working with high-finesse FP cavities; e.g., those that operate at radio frequencies (RF) [77].

To address systematic issues, the static signal can be modulated to finite frequency by rotating the cavity orientations with respect to the gradient. We also propose injecting multiple cavity-resonant frequencies to perform cavity co-metrology and break possible degeneracies with various chromatic systematic effects and noise sources.

Interferometric detection of axions is not a new idea. A similar experimental proposal for probing axion DM appears in Ref. [47]; see also Refs. [46, 48–51]. These proposals are, however, tailored to search for the dominant, temporal component of the DM axion gradient: $|\dot{\phi}|_{\text{DM}} \sim 2\times10^{-3}\,\text{eV}^2 \sim 10^3|\nabla\phi|_{\text{DM}}$. This is smaller than the largest allowed spatial gradient from an Earth-sourced axion, and does not have an intrinsic spatial directionality. For slowly varying DM axion fields, $m_\phi\ell \ll 1$, the latter fact leads to the round-trip signal cancellation mentioned above [47]; to overcome this for a DM axion, additional optical elements inside the cavity are required [47], or alternative experimental designs must be considered [48–51]. Moreover, a DM axion experiment has a bandwidth limitation arising from the virialized nature of DM [78–80]. Such a limitation is not present for a static, sourced axion field gradient, for which noise may thus be more efficiently averaged down.

Signal.—We consider the low-energy effective axion model (we work in natural units; $\hbar = c = 1$)

$$\mathcal{L} \supset \mathcal{L}_{\text{SM}} + \frac{1}{2}(\partial\phi)^2 - \frac{1}{2}m_\phi^2\phi^2 - \frac{g_{\phi\gamma}}{4}\phi F\widetilde{F} \\ - (\tilde{g}_B + \tilde{g}_{B-L})\phi\bar{N}N - (\tilde{g}_L - \tilde{g}_{B-L})\phi\bar{e}e\,, \tag{1}$$

where ϕ is the axion, F ($\widetilde{F}$) is the (dual) photon field-strength tensor, N is a nucleon, and e an electron. Consider an FP cavity of length ℓ and finesse $\mathcal{F}$ with its axis aligned to local vertical on the surface of Earth. External laser light with wavelength λ (wavenumber $k = 2\pi/\lambda$) is introduced to the FP cavity via the upper mirror. We model the lower (upper) mirror to be perfectly (highly) reflecting for light incident from the interior of the cavity, and both mirrors to be lossless.

Ignoring transverse spatial gradients in the beam profile, plane right (+) [respectively, left (−)] circularly polarized light incident on the exterior face of the upper mirror is reflected from that mirror as left [respectively, right] circularly polarized light with a phase shift $e^{i\alpha_+}$ [$e^{i\alpha_-}$], where

$$\tan\alpha_\pm = \frac{\pi\sqrt{4\mathcal{F}^2+\pi^2}\,\sin(2k\ell \pm g_{\phi\gamma}\Delta\phi)}{(2\mathcal{F}^2+\pi^2)\cos(2k\ell \pm g_{\phi\gamma}\Delta\phi) - 2\mathcal{F}^2}\,, \tag{2}$$

where $\Delta\phi \equiv \phi(\text{lower}) - \phi(\text{upper})$ is the difference in the axion field between the lower and upper mirrors.

For a cavity near longitudinal resonance, $\ell = \ell_n + \Delta\ell$ with $\ell_n = n\lambda/2$ ($n = 1, 2, \ldots$) and $|\Delta\ell| \ll \ell_n$, and in the combined limits $\alpha_\pm \ll 1$ and $\mathcal{F} \gg 1$, the phase shifts are

$$\alpha_\pm \approx \frac{2\mathcal{F}}{\pi}\left(2k\Delta\ell \pm g_{\phi\gamma}\Delta\phi\right). \tag{3}$$

For two cavities both run near resonance and driven with oppositely handed light, a static differential phase shift $\Delta\alpha \equiv \alpha_+ - \alpha_- = \Delta\alpha_\phi + \Delta\alpha_\ell$ develops, where

$$\Delta\alpha_\phi \equiv \frac{4\mathcal{F}}{\pi}\cdot g_{\phi\gamma}\Delta\phi\,, \tag{4}$$

$$\Delta\alpha_\ell \equiv \frac{4\mathcal{F}}{\pi}\cdot k\left(\Delta\ell_+ - \Delta\ell_-\right), \tag{5}$$

and where $\Delta\ell_\pm$ are the offsets from resonant length for the cavities driven with $\pm$-handed light. The axion signal $\Delta\alpha_\phi$ is a static, achromatic phase shift between the cavities, while a differential length fluctuation of the cavities causes a chromatic phase shift $\Delta\alpha_\ell = \Delta\alpha_\ell(\lambda)$.

To estimate $\Delta\phi$, we adopt a simplified model for Earth (radius $R_\oplus$), ignoring its internal structure and approximating it as a homogeneous, spherically symmetric body with baryon and lepton charges satisfying $B \approx 2L \approx M_\oplus/\mu_a$, where $M_\oplus$ is the mass of Earth and μ_a is the atomic mass unit. In this setup, the on-resonance axion-induced differential phase shift is

$$\Delta\alpha_\phi = \tilde{g}_\oplus g_{\phi\gamma}\frac{\mathcal{F}}{\pi^2}\frac{M_\oplus}{\mu_a}\frac{\ell\,e^{-m_\phi d}}{(R_\oplus+d)^2}\Psi(m_\phi\ell, m_\phi R_\oplus, m_\phi d)\,, \tag{6}$$

where d is the distance between the surface of Earth and the lower mirrors of the FP cavities (we take $d = 10\,\mathrm{cm}$ throughout), $\tilde{g}_\oplus \equiv \tilde{g}_B + \frac{1}{2}(\tilde{g}_{B-L} + \tilde{g}_L)$, and

$$\Psi(x,y,z) \equiv -\frac{3e^{-y}}{y^3}\,(y\cosh y - \sinh y) \times \frac{y+z}{x}\left[1 - \frac{e^{-x}}{1 + x/(y+z)}\right]. \tag{7}$$

Ψ accounts for $\phi(r)$ being sourced dominantly by those parts of Earth within the axion-field range r_ϕ [74, 81], and for the full r-dependence of $\phi(r)$. If $\ell, d \ll R_\oplus$, we have $\Delta\alpha_\phi \propto (m_\phi)^{-n}$ with $n = 0$ for $m_\phi \lesssim 1/R_\oplus$, and $n = 1$ for $1/R_\oplus \lesssim m_\phi \lesssim \min[1/\ell, 1/d]$. If $d < \ell$, then $n = 2$ for $1/\ell \lesssim m_\phi \lesssim 1/d$. For $m_\phi \gtrsim 1/d$, $\Delta\alpha_\phi \propto e^{-m_\phi d}$.

We envisage standard dark-port operation for the Michelson interferometer [82]: carrier-signal phase modulation creates sidebands displaced from FP cavity resonance that do not pick up a phase shift, whereas the carrier is tuned to FP cavity resonance and experiences the signal phase shift. Access to a linear signal is achieved in the beat note of the carrier and the sidebands at the beamsplitter, which can be mixed down for readout.

The signal at Eq. (6) is static, but if the orientation of the cavities is rotated from vertical about their midpoint at an angular frequency Ω, the signal is modulated up to finite frequency: $\Delta\alpha_\phi \to \Delta\alpha_\phi \cdot f(t)$, where, for $\ell \ll R_\oplus$,

$$f(t) \approx \frac{\sinh\left[\frac{m_\phi \ell}{2}\cos(\Omega t)\right]}{\sinh\left(\frac{m_\phi \ell}{2}\right)} \overset{m_\phi \ell \ll 1}{\longrightarrow} \cos(\Omega t)\,. \tag{8}$$

Were the cavities instead modulated at a frequency Ω by an angle $\pm\theta_0$ from vertical, $\Omega t \to \theta_0 \cos(\Omega t)$ in Eq. (8).

For sufficiently light axions ($m_\phi \lesssim 1/\mathrm{AU} \sim 10^{-18}\,\mathrm{eV}$), one could additionally search for the sub-leading axion gradient sourced by the Sun at Earth, $|\nabla\phi|_\odot \sim 10^{-4}\,\mathrm{eV}^2 \times \tilde{g}_B/(6\times 10^{-25})$ for $m_\phi \lesssim 1/(\mathrm{AU})$, that modulates direction at the period of a synodic day.

One can also consider using a small, laboratory mass to source a (much smaller) axion field gradient. For cavities in radial orientation around a homogeneous spherical source of radius R (with the nearest mirror of each FP cavity a distance d from the source surface), the signal is given by Eqs. (6) and (7) with replacements $R_\oplus \to R$ and $M_\oplus \tilde{g}_\oplus/\mu_a \to B\tilde{g}_B + L\tilde{g}_L + (B-L)\tilde{g}_{B-L}$. Other source geometries give similar results, up to geometrical factors. Importantly, in this setup, the cavities can be oriented horizontally, with modulation of the signal to non-zero frequency achieved either by moving the source mass (cf. Ref. [83]), or by rotating the cavities about a vertical axis (cf. Ref. [71]). This may have technical advantages over vertically oriented cavities being rotated about a horizontal axis to achieve modulation of the signal from the fixed, vertical Earth-sourced field gradient.

Reach.—A projection for the reach of this experiment to the axion signal requires understanding various stochastic noise sources and confounding systematics, and in some cases mitigating the latter.

Photon shot noise statistically limits interferometer sensitivity. Suppose we integrate coherently for a time τ; the expected number of photons arriving at the interferometer beamsplitter, where the interference pattern is observed, is $N_\gamma = P_0\tau/\omega$, where $P_0 \sim \pi P_{\mathrm{cav}}/(2\mathcal{F})$ is the average power incident on the beamsplitter if P_{cav} is the circulating FP cavity power, and $\omega = 2\pi/\lambda$ is the angular frequency of the light. The phase uncertainty is then $\sim 1/\sqrt{N_\gamma}$. We estimate that the signal-to-noise ratio (SNR) for shot noise is

$$\mathrm{SNR}_{\mathrm{shot}} \sim \sqrt{\frac{2\pi P_{\mathrm{cav}}\tau}{\omega\mathcal{F}}}\,\Delta\alpha_\phi\,. \tag{9}$$

For all our projections, we take $\tau = 300\,\mathrm{days}$ and fix $P_{\mathrm{cav}} = 1\,\mathrm{MW}$, adjusting P_0 depending on $\mathcal{F}$.

In distinct contrast to an architecture optimized for gravitational-wave detection, the mirrors at the ends of the FP cavities in our proposal should be attached rigidly to a structure instead of being isolated; a high mechanical-resonance frequency for this support structure will suppress radiation-pressure noise. Modeling the cavity system as being embedded in a rigid block of mass M with fundamental vibrational frequency ω_{vib}, we can estimate the SNR due to radiation pressure noise as

$$\mathrm{SNR}_{\mathrm{rad}} \sim \frac{\pi}{2\sqrt{2}}\frac{M\omega_{\mathrm{vib}}^2}{\mathcal{F}^{3/2}}\sqrt{\frac{\tau}{P_{\mathrm{cav}}\omega^3}}\,\Delta\alpha_\phi\,. \tag{10}$$

We take the block to be cubic, with side-length ℓ_{sys}, constant density $\rho_{\mathrm{cav}} \sim 8\,\mathrm{g/cm}^3$, and sound speed $c_s \sim 6\,\mathrm{km/s}$, and we estimate $\omega_{\mathrm{vib}} \sim \pi c_s/\ell_{\mathrm{sys}}$.

For a cavity system at finite temperature there will also be thermal vibrational noise leading to fluctuating cavity lengths. Taking the same cavity-system model as above, we use the fluctuation–dissipation theorem to estimate

$$\mathrm{SNR}_{\mathrm{vib}} \sim \frac{\pi}{4}\sqrt{\frac{\tau M Q_{\mathrm{vib}}\omega_{\mathrm{vib}}^3}{T_{\mathrm{sys}}}}\frac{\Delta\alpha_\phi}{\omega\mathcal{F}}\,, \tag{11}$$

where T_{sys} is the system temperature and Q_{vib} is the mechanical-resonance quality factor. We assume cryogenic operation, $T_{\mathrm{sys}} \sim 4\,\mathrm{K}$, and take $Q_{\mathrm{vib}} \sim 10^3$. Thermal readout noise for an RF system (estimated via the Dicke radiometer equation) is subdominant.

If both cavities are embedded in the same rigid structure, some common length-fluctuation noise could cancel (see also Ref. [47]), increasing both $\mathrm{SNR}_{\mathrm{rad}}$ and $\mathrm{SNR}_{\mathrm{vib}}$.

The total SNR may be estimated as

$$\frac{1}{(\mathrm{SNR}_{\mathrm{tot}})^2} = \sum_i \frac{1}{(\mathrm{SNR}_i)^2}. \tag{12}$$

In Fig. 2, we show $\mathrm{SNR}_{\mathrm{tot}} = 1$ (dashed lines) and $\mathrm{SNR}_{\mathrm{shot}} = 1$ (solid lines) reach estimates for the product of couplings $\tilde{g}_B g_{\phi\gamma}$ for three different experimental

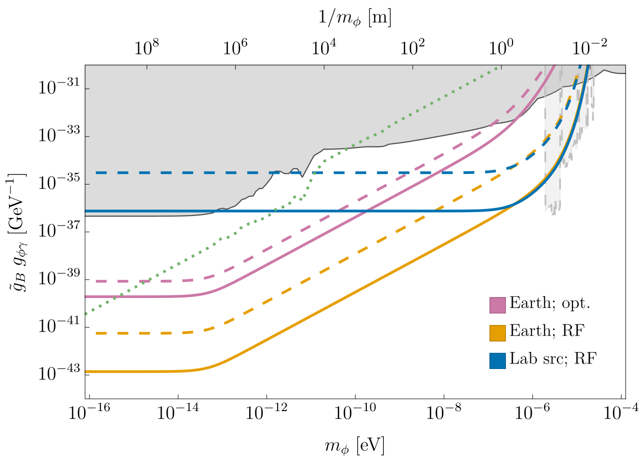

FIG. 2. Projected reach curves at SNR of 1 for various experimental architectures: (1) Earth as a source and a laser-based cavity search (purple); (2) Earth as a source and an RF-based cavity search (orange); and (3) a laboratory source and an RF-based cavity search (blue). Dashed lines are limited by vibrational noise at finite temperature [Eq. (11)]; solid lines take into account only shot noise [Eq. (9)]. The scaling with m_ϕ is explained below Eq. (7). Parameters are discussed in the text; see also Tab. I. The dark-grey region is ruled out by fifth-force constraints on $\tilde{g}_B$ [69–76], and various astrophysical constraints on $g_{\phi\gamma}$ [58–67]. The light-grey shaded region would be excluded were the axion also the DM [84–90]. Above the dotted green line, an axion mass tuning may be required, assuming $\Lambda = 10\,\mathrm{TeV}$ and $g_{\phi\gamma}$ fixed at current limits.

architectures, using the optical or open RF cavity interferometer parameters shown in Tab. I: (1) Earth as the axion source, with the optical interferometer setup; (2) Earth as the axion source, with the RF interferometer setup; and (3) a small laboratory-mass axion source (radius $R = 1\,\mathrm{m}$, density $\rho = 8\,\mathrm{g/cm^3}$), with the RF interferometer setup. In making these projections, we set $\tilde{g}_L = \tilde{g}_{B-L} = 0$; current constraints and signal-reach estimates for cases with these couplings non-zero are broadly similar to those for $\tilde{g}_B$, up to $\mathcal{O}(3)$ numerical factors. Note that the lab-sourced axion gradient in case (3) is far weaker than that for Earth, $|\nabla\phi|_{\mathrm{src}}(r = R) \sim 2\times10^{-7}|\nabla\phi|_\oplus$ for $m_\phi R_\oplus \lesssim 1$; it is also significantly weaker than the naturally modulating solar source, but the latter is only detectable for $m_\phi \lesssim 10^{-18}\,\mathrm{eV}$. For a homogeneous source, $\Delta\alpha_\phi \propto \rho R$ for $m_\phi R \ll 1$; tradespace thus exists to optimize for lab-source size and/or density.

Fig. 2 also shows where the axion bare mass may need to be tuned against the quantum correction $\delta m^2 \sim \tilde{g}_B^2\Lambda^2/(8\pi^2)$, where Λ is a UV cutoff scale, to maintain a light axion, assuming that $g_{\phi\gamma}$ is fixed at current bounds.

Discussion.—The achromatic axion phase shift can be distinguished from chromatic noise arising from differential cavity-length fluctuations. Running each cavity with multiple cavity-resonant frequencies of light simultaneously could thus suppress chromatic backgrounds; this differs from a GW detector, where the signal is degenerate with a differential length fluctuation. Such multi-frequency 'co-metrology' techniques (cf., e.g., Refs. [91, 92]) could allow the mitigation of vibrational and radiation-pressure noise backgrounds for the signal to the level of the shot-noise floor; we thus also show reach projections in Fig. 2 limited by shot noise only. Further investigation of this technique is warranted.

TABLE I. Experimental parameters, as defined in the text, assumed for the optical or open radio-frequency (RF) Fabry–Pérot interferometer reach projections. We adopt as parameters for the RF system those demonstrated in Ref. [77].

Parameter	Optical	RF
$\omega/2\pi$	$1/(1064\,\mathrm{nm})$	$51\,\mathrm{GHz}$
$\mathcal{F}$	10^4	4.6×10^9
ℓ [m]	1	0.027
ℓ_{sys} [m]	1	0.3

We also note that there is a potential systematic for the measurement: cavities have a degree of intrinsic circular birefringence; see, e.g., Refs. [93–95]. This strongly motivates signal modulation: only variations in the cavity birefringence properties at the modulation frequency Ω are then relevant (including possible changes in stress-induced birefringence were the cavities to be rotated in Earth's gravitational field). Moreover, the multi-frequency techniques noted above would also assist in breaking degeneracy with the signal, as intrinsic birefringence will be chromatic. Additionally, running the cavity at multiple different lengths ℓ could break degeneracy between our signal $\Delta\alpha_\phi \propto \ell$, and any ℓ-independent phase shift due to mirror coatings or abnormalities. However, because cavity birefringence depends in detail on the properties of the optical or RF elements in the cavity, we defer study of this issue to future technical work.

In addition to the open RF FP cavities we considered in this work, another possible experimental architecture would use closed superconducting radio-frequency (SRF) cavity resonators (see, e.g., Refs. [96, 97]) in the interferometer arms. However, finite machining tolerances of the cavity walls appear to limit the fidelity with which opposite circular polarizations propagate without mixing, limiting the usable cavity finesse to well below that attainable for the highest-Q SRF cavities [$\mathcal{F} = (\omega_{\mathrm{FSR}}/\omega_n)Q$, where Q is the cavity quality factor, ω_{FSR} is the cavity free spectral range, and ω_n is the cavity resonance frequency].

In this paper, we have proposed a novel interferometric experiment to search for static axion field gradients. Provided that shot-noise-limited sensitivity can be reached, an approach exploiting open, high-finesse RF FP resonators could allow the exploration of ~ 6 orders of magnitude of new parameter space beyond current limits on the product coupling $\tilde{g}_Q g_{\phi\gamma}$ for $m_\phi \lesssim 10^{-10}\,\mathrm{eV}$.

We thank William DeRocco, Anson Hook, Xuheng Luo, Anubhav Mathur, and Oleksandr S. Melnychuk for useful discussions. This work was supported by the U.S. Department of Energy (DOE), Office of Science, National Quantum Information Science Research Centers, Superconducting Quantum Materials and Systems Center (SQMS) under Contract No. DE-AC02-07CH11359. Fermilab is operated by the Fermi Research Alliance, LLC under Contract No. DE-AC02-07CH11359 with the DOE. D.E.K. and S.R. are supported in part by the U.S. National Science Foundation (NSF) under Grant No. PHY-1818899. S.R. is also supported by the DOE under a QuantISED grant for MAGIS. The work of S.R. and M.A.F. was also supported by the Simons Investigator Award No. 827042. M.A.F. gratefully acknowledges the hospitality of the Simons Center for Geometry and Physics at Stony Brook University, where part of this work was undertaken. J.O.T. would like to thank the Kavli Institute for the Physics and Mathematics of the Universe for hospitality during the completion of this work.

* mfedderke@jhu.edu; author contributed equally.
† jedidiah@stanford.edu; author contributed equally.

[1] R. Peccei and H. R. Quinn, *CP Conservation in the Presence of Instantons*, Phys. Rev. Lett. **38** (1977) 1440–1443.
[2] S. Weinberg, *A New Light Boson?*, Phys. Rev. Lett. **40** (1978) 223–226.
[3] F. Wilczek, *Problem of Strong P and T Invariance in the Presence of Instantons*, Phys. Rev. Lett. **40** (1978) 279–282.
[4] J. A. Frieman, C. T. Hill, A. Stebbins and I. Waga, *Cosmology with ultralight pseudo Nambu-Goldstone bosons*, Phys. Rev. Lett. **75** (1995) 2077–2080 [arXiv:astro-ph/9505060].
[5] R. R. Caldwell, R. Dave and P. J. Steinhardt, *Cosmological imprint of an energy component with general equation of state*, Phys. Rev. Lett. **80** (1998) 1582–1585 [arXiv:astro-ph/9708069].
[6] L. D. Duffy and K. van Bibber, *Axions as Dark Matter Particles*, New J. Phys. **11** (2009) 105008 [arXiv:0904.3346].
[7] L. Hui, J. P. Ostriker, S. Tremaine and E. Witten, *Ultralight scalars as cosmological dark matter*, Phys. Rev. D **95** (2017) 043541 [arXiv:1610.08297].
[8] P. Svrcek and E. Witten, *Axions In String Theory*, JHEP **06** (2006) 051 [arXiv:hep-th/0605206].
[9] A. Arvanitaki, S. Dimopoulos, S. Dubovsky, N. Kaloper and J. March-Russell, *String Axiverse*, Phys. Rev. D **81** (2010) 123530 [arXiv:0905.4720].
[10] S. M. Carroll, G. B. Field and R. Jackiw, *Limits on a Lorentz and Parity Violating Modification of Electrodynamics*, Phys. Rev. D **41** (1990) 1231.
[11] S. M. Carroll and G. B. Field, *Einstein equivalence principle and the polarization of radio galaxies*, Phys. Rev. D **43** (1991) 3789–3793.
[12] D. Harari and P. Sikivie, *Effects of a Nambu-Goldstone boson on the polarization of radio galaxies and the cosmic microwave background*, Phys. Lett. B **289** (1992) 67–72.
[13] S. M. Carroll, *Quintessence and the rest of the world*, Phys. Rev. Lett. **81** (1998) 3067–3070 [arXiv:astro-ph/9806099].
[14] A. Lue, L. Wang and M. Kamionkowski, *Cosmological signature of new parity-violating interactions*, Phys. Rev. Lett. **83** (1999) 1506–1509 [arXiv:astro-ph/9812088].
[15] G.-C. Liu, S. Lee and K.-W. Ng, *Effect on cosmic microwave background polarization of coupling of quintessence to pseudoscalar formed from the electromagnetic field and its dual*, Phys. Rev. Lett. **97** (2006) 161303 [arXiv:astro-ph/0606248].
[16] W.-T. Ni, *From Equivalence Principles to Cosmology: Cosmic Polarization Rotation, CMB Observation, Neutrino Number Asymmetry, Lorentz Invariance and CPT*, Prog. Theor. Phys. Suppl. **172** (2008) 49–60 [arXiv:0712.4082].
[17] M. Pospelov, A. Ritz and C. Skordis, *Pseudoscalar perturbations and polarization of the cosmic microwave background*, Phys. Rev. Lett. **103** (2009) 051302 [arXiv:0808.0673].
[18] F. Finelli and M. Galaverni, *Rotation of Linear Polarization Plane and Circular Polarization from Cosmological Pseudo-Scalar Fields*, Phys. Rev. D **79** (2009) 063002 [arXiv:0802.4210].
[19] M. Galaverni and F. Finelli, *Rotation of linear polarization plane from cosmological pseudoscalar fields*, Nucl. Phys. Proc. Suppl. **194** (2009) 51–56.
[20] R. R. Caldwell, V. Gluscevic and M. Kamionkowski, *Cross-correlation of cosmological birefringence with CMB temperature*, Phys. Rev. D **84** (2011) 043504 [arXiv:1104.1634].
[21] V. Gluscevic, D. Hanson, M. Kamionkowski and C. M. Hirata, *First CMB constraints on direction-dependent cosmological birefringence from WMAP-7*, Phys. Rev. D **86** (2012) 103529 [arXiv:1206.5546].
[22] M. Li and B. Yu, *New Constraints on Anisotropic Rotation of CMB Polarization*, JCAP **06** (2013) 016 [arXiv:1303.1881].
[23] S. Lee, G.-C. Liu and K.-W. Ng, *Imprint of Scalar Dark Energy on Cosmic Microwave Background Polarization*, Phys. Rev. D **89** (2014) 063010 [arXiv:1307.6298].
[24] G. Gubitosi, M. Martinelli and L. Pagano, *Including birefringence into time evolution of CMB: current and future constraints*, JCAP **12** (2014) 020 [arXiv:1410.1799].
[25] M. Galaverni, G. Gubitosi, F. Paci and F. Finelli, *Cosmological birefringence constraints from CMB and astrophysical polarization data*, JCAP **08** (2015) 031 [arXiv:1411.6287].
[26] A. Gruppuso, M. Gerbino, P. Natoli, L. Pagano, N. Mandolesi, A. Melchiorri et al., *Constraints on cosmological birefringence from Planck and BICEP2/Keck data*, JCAP **06** (2016) 001 [arXiv:1509.04157].
[27] Planck Collaboration, N. Aghanim et al., *Planck intermediate results. XLIX. Parity-violation constraints from polarization data*, Astron. Astrophys. **596** (2016) A110 [arXiv:1605.08633].
[28] G. Sigl and P. Trivedi, *Axion-like Dark Matter Constraints from CMB Birefringence*, arXiv:1811.07873.
[29] M. A. Fedderke, P. W. Graham and S. Rajendran, *Axion Dark Matter Detection with CMB Polarization*, Phys. Rev. D **100** (2019) 015040 [arXiv:1903.02666].
[30] P. Agrawal, A. Hook and J. Huang, *A CMB Millikan*

experiment with cosmic axiverse strings, *JHEP* **07** (2020) 138 [arXiv:1912.02823].

[31] A. Gruppuso, D. Molinari, P. Natoli and L. Pagano, *Planck 2018 constraints on anisotropic birefringence and its cross-correlation with CMB anisotropy*, *JCAP* **11** (2020) 066 [arXiv:2008.10334].

[32] M. Jain, A. J. Long and M. A. Amin, *CMB birefringence from ultralight-axion string networks*, *JCAP* **05** (2021) 055 [arXiv:2103.10962].

[33] BICEP/Keck Collaboration, P. A. R. Ade et al., *BICEP/Keck XIV: Improved constraints on axionlike polarization oscillations in the cosmic microwave background*, *Phys. Rev. D* **105** (2022) 022006 [arXiv:2108.03316].

[34] M. Jain, R. Hagimoto, A. J. Long and M. A. Amin, *Searching for axion-like particles through CMB birefringence from string-wall networks*, *JCAP* **10** (2022) 090 [arXiv:2208.08391].

[35] J. R. Eskilt and E. Komatsu, *Improved constraints on cosmic birefringence from the WMAP and Planck cosmic microwave background polarization data*, *Phys. Rev. D* **106** (2022) 063503 [arXiv:2205.13962].

[36] M. Bortolami, M. Billi, A. Gruppuso, P. Natoli and L. Pagano, *Planck constraints on cross-correlations between anisotropic cosmic birefringence and CMB polarization*, *JCAP* **09** (2022) 075 [arXiv:2206.01635].

[37] P. Diego-Palazuelos et al., *Cosmic Birefringence from the Planck Data Release 4*, *Phys. Rev. Lett.* **128** (2022) 091302 [arXiv:2201.07682].

[38] SPT-3G Collaboration, K. R. Ferguson et al., *Searching for axionlike time-dependent cosmic birefringence with data from SPT-3G*, *Phys. Rev. D* **106** (2022) 042011 [arXiv:2203.16567].

[39] M. Galaverni, F. Finelli and D. Paoletti, *Redshift evolution of cosmic birefringence in CMB anisotropies*, arXiv:2301.07971.

[40] POLARBEAR Collaboration, S. Adachi et al., *Constraints on axion-like polarization oscillations in the cosmic microwave background with POLARBEAR*, arXiv:2303.08410.

[41] S. di Serego Alighieri, F. Finelli and M. Galaverni, *Limits on Cosmological Birefringence from the UV Polarization of Distant Radio Galaxies*, *Astrophys. J.* **715** (2010) 33–38 [arXiv:1003.4823].

[42] T. Fujita, R. Tazaki and K. Toma, *Hunting Axion Dark Matter with Protoplanetary Disk Polarimetry*, *Phys. Rev. Lett.* **122** (2019) 191101 [arXiv:1811.03525].

[43] M. M. Ivanov, Y. Y. Kovalev, M. L. Lister, A. G. Panin, A. B. Pushkarev, T. Savolainen et al., *Constraining the photon coupling of ultra-light dark-matter axion-like particles by polarization variations of parsec-scale jets in active galaxies*, *JCAP* **02** (2019) 059 [arXiv:1811.10997].

[44] T. Liu, G. Smoot and Y. Zhao, *Detecting axionlike dark matter with linearly polarized pulsar light*, *Phys. Rev. D* **101** (2020) 063012 [arXiv:1901.10981].

[45] T. Liu, X. Lou and J. Ren, *Pulsar Polarization Arrays*, *Phys. Rev. Lett.* **130** (2023) 121401 [arXiv:2111.10615].

[46] A. C. Melissinos, *Search for Cosmic Axions using an Optical Interferometer*, *Phys. Rev. Lett.* **102** (2009) 202001 [arXiv:0807.1092].

[47] W. DeRocco and A. Hook, *Axion interferometry*, *Phys. Rev. D* **98** (2018) 035021 [arXiv:1802.07273].

[48] I. Obata, T. Fujita and Y. Michimura, *Optical Ring Cavity Search for Axion Dark Matter*, *Phys. Rev. Lett.* **121** (2018) 161301 [arXiv:1805.11753].

[49] H. Liu, B. D. Elwood, M. Evans and J. Thaler, *Searching for Axion Dark Matter with Birefringent Cavities*, *Phys. Rev. D* **100** (2019) 023548 [arXiv:1809.01656].

[50] D. Martynov and H. Miao, *Quantum-enhanced interferometry for axion searches*, *Phys. Rev. D* **101** (2020) 095034 [arXiv:1911.00429].

[51] Y. Oshima, H. Fujimoto, J. Kume, S. Morisaki, K. Nagano, T. Fujita et al., *First Results of Axion Dark Matter Search with DANCE*, arXiv:2303.03594.

[52] J. E. Moody and F. Wilczek, *New macroscopic forces?*, *Phys. Rev. D* **30** (1984) 130–138.

[53] M. Pospelov, *CP odd interaction of axion with matter*, *Phys. Rev. D* **58** (1998) 097703 [arXiv:hep-ph/9707431].

[54] H. Davoudiasl and R. Szafron, *Muon $g-2$ and a Geocentric New Field*, arXiv:2210.14959.

[55] P. Agrawal, D. E. Kaplan, O. Kim, S. Rajendran and M. Reig, *Searching for axion forces with precision precession in storage rings*, arXiv:2210.17547.

[56] G. Raffelt and L. Stodolsky, *Mixing of the photon with low-mass particles*, *Phys. Rev. D* **37** (1988) 1237–1249.

[57] G. G. Raffelt, *Stars as Laboratories for Fundamental Physics: The Astrophysics of Neutrinos, Axions, and Other Weakly Interacting Particles*. University of Chicago Press, 1996.

[58] D. Wouters and P. Brun, *Constraints on Axion-like Particles from X-Ray Observations of the Hydra Galaxy Cluster*, *Astrophys. J.* **772** (2013) 44 [arXiv:1304.0989].

[59] M. C. D. Marsh, H. R. Russell, A. C. Fabian, B. P. McNamara, P. Nulsen and C. S. Reynolds, *A New Bound on Axion-Like Particles*, *JCAP* **12** (2017) 036 [arXiv:1703.07354].

[60] C. S. Reynolds, M. C. D. Marsh, H. R. Russell, A. C. Fabian, R. Smith, F. Tombesi et al., *Astrophysical limits on very light axion-like particles from Chandra grating spectroscopy of NGC 1275*, *Astrophys. J.* **890** (2020) 59 [arXiv:1907.05475].

[61] J. S. Reynés, J. H. Matthews, C. S. Reynolds, H. R. Russell, R. N. Smith and M. C. D. Marsh, *New constraints on light axion-like particles using Chandra transmission grating spectroscopy of the powerful cluster-hosted quasar H1821+643*, *Mon. Not. Roy. Astron. Soc.* **510** (2021) 1264–1277 [arXiv:2109.03261].

[62] C. Dessert, D. Dunsky and B. R. Safdi, *Upper limit on the axion-photon coupling from magnetic white dwarf polarization*, *Phys. Rev. D* **105** (2022) 103034 [arXiv:2203.04319].

[63] J. Jaeckel, P. C. Malta and J. Redondo, *Decay photons from the axionlike particles burst of type II supernovae*, *Phys. Rev. D* **98** (2018) 055032 [arXiv:1702.02964].

[64] S. Hoof and L. Schulz, *Updated constraints on axion-like particles from temporal information in supernova SN1987A gamma-ray data*, *JCAP* **03** (2023) 054 [arXiv:2212.09764].

[65] A. Payez, C. Evoli, T. Fischer, M. Giannotti, A. Mirizzi and A. Ringwald, *Revisiting the SN1987A gamma-ray limit on ultralight axion-like particles*, *JCAP* **02** (2015) 006 [arXiv:1410.3747].

[66] A. Ayala, I. Domínguez, M. Giannotti, A. Mirizzi and O. Straniero, *Revisiting the bound on axion-photon coupling from Globular Clusters*, *Phys. Rev. Lett.* **113** (2014) 191302 [arXiv:1406.6053].

[67] M. J. Dolan, F. J. Hiskens and R. R. Volkas, *Advancing globular cluster constraints on the axion-photon coupling*, *JCAP* **10** (2022) 096 [arXiv:2207.03102].

[68] C. O'Hare, *cajohare/AxionLimits*, https://cajohare.github.io/AxionLimits/. 10.5281/zenodo.3932430.

[69] S. Schlamminger, K. Y. Choi, T. A. Wagner, J. H. Gundlach and E. G. Adelberger, *Test of the equivalence principle using a rotating torsion balance*, Phys. Rev. Lett. **100** (2008) 041101 [arXiv:0712.0607].

[70] E. Adelberger, J. Gundlach, B. Heckel, S. Hoedl and S. Schlamminger, *Torsion balance experiments: A low-energy frontier of particle physics*, Prog. Part. Nucl. Phys. **62** (2009) 102–134.

[71] T. A. Wagner, S. Schlamminger, J. H. Gundlach and E. G. Adelberger, *Torsion-balance tests of the weak equivalence principle*, Class. Quant. Grav. **29** (2012) 184002 [arXiv:1207.2442].

[72] P. Touboul et al., *MICROSCOPE Mission: Final Results of the Test of the Equivalence Principle*, Phys. Rev. Lett. **129** (2022) 121102 [arXiv:2209.15487].

[73] P. Touboul et al., *MICROSCOPE Mission: First Results of a Space Test of the Equivalence Principle*, Phys. Rev. Lett. **119** (2017) 231101 [arXiv:1712.01176].

[74] J. Bergé, P. Brax, G. Métris, M. Pernot-Borràs, P. Touboul and J.-P. Uzan, *MICROSCOPE Mission: First Constraints on the Violation of the Weak Equivalence Principle by a Light Scalar Dilaton*, Phys. Rev. Lett. **120** (2018) 141101 [arXiv:1712.00483].

[75] E. A. Shaw, M. P. Ross, C. A. Hagedorn, E. G. Adelberger and J. H. Gundlach, *Torsion-balance search for ultralow-mass bosonic dark matter*, Phys. Rev. D **105** (2022) 042007 [arXiv:2109.08822].

[76] M. A. Fedderke and A. Mathur, *Asteroids for ultralight dark-photon dark-matter detection*, Phys. Rev. D **107** (2023) 043004 [arXiv:2210.09324].

[77] S. Kuhr, S. Gleyzes, C. Guerlin, J. Bernu, U. B. Hoff, S. Deléglise et al., *Ultrahigh finesse Fabry-Pérot superconducting resonator*, Appl. Phys. Lett. **90** (2007) 164101 [arXiv:quant-ph/0612138].

[78] J. W. Foster, N. L. Rodd and B. R. Safdi, *Revealing the Dark Matter Halo with Axion Direct Detection*, Phys. Rev. D **97** (2018) 123006 [arXiv:1711.10489].

[79] G. P. Centers et al., *Stochastic fluctuations of bosonic dark matter*, Nat. Commun. **12** (2021) 7321 [arXiv:1905.13650].

[80] D. F. Jackson Kimball, L. D. Duffy and D. J. E. Marsh, *Ultralight Bosonic Dark Matter Theory*, in *The Search for Ultralight Bosonic Dark Matter* (D. F. Jackson Kimball and K. van Bibber, eds.), pp. 31–72. Springer, 2023. DOI.

[81] E. G. Adelberger, B. R. Heckel and A. E. Nelson, *Tests of the gravitational inverse square law*, Ann. Rev. Nucl. Part. Sci. **53** (2003) 77–121 [arXiv:hep-ph/0307284].

[82] M. Maggiore, *Gravitational Waves. Volume 1: Theory and Experiments*. Oxford University Press, Oxford, 2008.

[83] A. Arvanitaki and A. A. Geraci, *Resonantly Detecting Axion-Mediated Forces with Nuclear Magnetic Resonance*, Phys. Rev. Lett. **113** (2014) 161801 [arXiv:1403.1290].

[84] S. DePanfilis, A. C. Melissinos, B. E. Moskowitz, J. T. Rogers, Y. K. Semertzidis, W. U. Wuensch et al., *Limits on the abundance and coupling of cosmic axions at* $4.5 < m_a < 5.0\ \mu eV$, Phys. Rev. Lett. **59** (1987) 839–842.

[85] ADMX Collaboration, S. J. Asztalos et al., *A SQUID-based microwave cavity search for dark-matter axions*, Phys. Rev. Lett. **104** (2010) 041301 [arXiv:0910.5914].

[86] ADMX Collaboration, N. Du et al., *A Search for Invisible Axion Dark Matter with the Axion Dark Matter Experiment*, Phys. Rev. Lett. **120** (2018) 151301 [arXiv:1804.05750].

[87] ADMX Collaboration, C. Boutan et al., *Piezoelectrically Tuned Multimode Cavity Search for Axion Dark Matter*, Phys. Rev. Lett. **121** (2018) 261302 [arXiv:1901.00920].

[88] ADMX Collaboration, T. Braine et al., *Extended Search for the Invisible Axion with the Axion Dark Matter Experiment*, Phys. Rev. Lett. **124** (2020) 101303 [arXiv:1910.08638].

[89] ADMX Collaboration, C. Bartram et al., *Search for Invisible Axion Dark Matter in the 3.3–4.2* μ*eV Mass Range*, Phys. Rev. Lett. **127** (2021) 261803 [arXiv:2110.06096].

[90] ADMX Collaboration, C. Bartram et al., *Dark Matter Axion Search Using a Josephson Traveling Wave Parametric Amplifier*, arXiv:2110.10262.

[91] M. S. Safronova, D. Budker, D. DeMille, D. F. J. Kimball, A. Derevianko and C. W. Clark, *Search for New Physics with Atoms and Molecules*, Rev. Mod. Phys. **90** (2018) 025008 [arXiv:1710.01833].

[92] W. A. Terrano and M. V. Romalis, *Comagnetometer probes of dark matter and new physics*, Quantum Sci. Technol. **7** (2022) 014001 [arXiv:2106.09210].

[93] J. L. Hall, J. Ye and L.-S. Ma, *Measurement of mirror birefringence at the sub-ppm level: Proposed application to a test of QED*, Phys. Rev. A **62** (2000) 013815.

[94] A. J. Fleisher, D. A. Long, Q. Liu and J. T. Hodges, *Precision interferometric measurements of mirror birefringence in high-finesse optical resonators*, Phys. Rev. A **93** (2016) 013833.

[95] A. Ejlli, F. Della Valle and G. Zavattini, *Polarisation dynamics of a birefringent Fabry-Pérot cavity*, Appl. Phys. B **124** (2018) 22 [arXiv:1707.02967].

[96] H. S. Padamsee, *Superconducting radio-frequency cavities*, Ann. Rev. Nucl. Part. Sci. **64** (2014) 175–196.

[97] A. Romanenko et al., *New Exclusion Limit for Dark Photons from an SRF Cavity-Based Search (Dark SRF)*, arXiv:2301.11512.